DOE/ET-53088-596 IFSR #596

Percolation and Turbulent Diffusion: Transport on and Around Percolation Clusters

M.B. ISICHENKO
Institute for Fusion Studies
The University of Texas at Austin
Austin, Texas 78712

March 1993

PERCOLATION AND TURBULENT DIFFUSION: TRANSPORT ON AND AROUND PERCOLATION CLUSTERS*

M.B. Isichenko

Institute for Fusion Studies
The University of Texas at Austin
Austin, Texas 78712, U.S.A.

Abstract. A brief review of percolation theory is given and some of its novel applications are described. There are several continuum generalizations of the lattice percolation problem, of which the main emphasis is given to the "potential model," describing the statistics of the contour lines of a random potential, objects studied in the framework of "statistical topography." The variety of new physical applications come from the idea that many transport processes in turbulent and random media (fluids, plasmas, semiconductors, 2D electron gas, etc.) occur along the contours of some random potential. The simplest and the most fundamental example of this sort is the diffusion of a passive tracer in an incompressible two-dimensional flow, whose streamlines are the isolines of a random stream function. In the limit of a large Péclet number P, the effective diffusion in such a flow scales with P as the universal power of 10/13, expressable through the percolation critical exponents. More elaborate examples, where the transport scalings can be also obtained analytically, involve the plasma heat conduction in a stochastic magnetic field and/or electrostatic turbulence, the average conductivity of randomly inhomogeneous conductors, and the quantum Hall effect. A special section is devoted to reviewing the Dykhne reciprocity technique, applicable to two-dimensional, two-phase systems at the percolation threshold, where the effective transport coefficients can be calculated exactly.

1. Introduction

The percolation problem describes the simplest possible phase transition with nontrivial critical behavior. The pure geometrical nature of this transition and its compelling ap-

*Invited talk presented at the "Interdisciplinary Workshop on Statistical Description of Transport in Plasma, Astro- and Nuclear Physics," Les Houches, France, Feb. 2-11, 1993.

plication to diverse physical problems have drawn the attention of many researchers and the percolation theory is well reviewed [1—4]. The general formulation of the percolation problem is concerned with elementary geometrical objects such as spheres, sites, bonds, etc., placed at random in a d-dimensional lattice or continuum. The objects have a well-defined connectivity radius λ_0, and two objects are said to communicate if the distance between them is less than λ_0. One is interested in how many objects can form a cluster of communication and, especially, when and how the clusters become infinite. The control parameter of the problem is the density n_0 of the objects (their average number per unit volume), or the dimensionless site occupation probability $p = n_0\lambda_0^d$. The *percolation threshold*, $p = p_c$, corresponds to the minimum concentration at which an *infinite cluster* spans the space. Thus the percolation model exhibits two essential features: critical behavior and long-range correlations near the critical value of the control parameter p.

This model is relevant for a number of transport problems in disordered media exhibiting critical behavior, such as electron localization [5,6] and hopping conduction in amorphous solids [3,7]. These problems have long been among "traditional" applications of percolation theory, where the clusters are meant as the transport agents, thereby motivating numerous studies of transport *on* percolation clusters [8,9].

Not only critical phenomena can be associated with the percolation model. Consider, for example, the diffusion of a passively advected tracer in a two-dimensional, steady, incompressible random flow

$$\mathbf{v}(x,y) = \nabla\psi(x,y) \times \hat{\mathbf{z}} \,, \tag{1}$$

where $\psi(x,y)$ is a random stream function and $\hat{\mathbf{z}}$ a unit vector in the z direction. The streamlines of this flow are the contours of ψ. The geometry of the streamlines is associated with the geometry of percolation clusters as follows. Let us call "objects" the regions where $\psi(x,y)$ is less than a specified constant level h. If $z = \psi(x,y)$ is imagined to be the elevation of a random landscape and h designates the level of flooding, then the objects are the lakes. Two neighboring lakes are said to communicate if they merge into a bigger lake, thereby producing a cluster. So the contours $\psi(x,y) = h$ present the coastlines of the lakes, that is, the envelopes of the clusters. The control parameter of this percolation problem is the level h such that at some critical level, $h = h_c$, the lakes form an infinite ocean and among the contours $\psi(x,y) = h_c$ there is one infinitely long (Sec. 2).

Flow (1), however, includes streamlines lying at all levels, and its transport properties show no critical behavior in the only relevant control parameter, namely the Péclet number

$$P = \frac{\psi_0}{D_0} \,, \tag{2}$$

the ratio of the root-mean-square stream function and the molecular diffusivity of the tracer. Nevertheless, if the Péclet number is large, $P \gg 1$, the transport shows long correlation because the tracer particles advected along very large streamlines diffuse from these lines to more typical short closed lines very slowly and hence provide a significant *coherent* contribution to the turbulent diffusivity D^*. The larger the Péclet number, the longer and narrower the bundles of streamlines which dominate the effective transport

in the considered flow. Under certain constraints, the effective diffusivity scales as

$$D^* \simeq D_0 P^{10/13} , \quad P \gg 1 , \tag{3}$$

where the exponent 10/13 is expressable in terms of the critical exponents of two-dimensional percolation theory (Sec. 3).

The effective diffusion in a random flow presents an example of a long-range correlated phenomenon without critical behavior. The critical exponents of the percolation transition enter the result because the large value of the control parameter ($P \gg 1$) highlights a near-critical (in the sense of the contour percolation) set of streamlines dominating the effective transport. Unlike transport processes occurring *on* percolation clusters, the motion along incompressible streamlines represents transport *around* percolation clusters. It turns out even easier to study this type of transport processes, because the universality class of percolation perimeters is simpler than that of clusters themselves.

The appearance of formula (3) leaves little hope for its derivation using a regular perturbation theory method in solving the underlying advection-diffusion equation

$$\frac{\partial n}{\partial t} + \mathbf{v} \cdot \boldsymbol{\nabla} n = D_0 \nabla^2 n \tag{4}$$

for the tracer density n. Instead, geometrical arguments can be used to reduce the advection-diffusion problem to the problem of random contours, whose critical behavior is not amenable to any kind of a perturbation analysis but is well described in terms of percolation theory.

The flows discussed in the context of advection-diffusion are not necessarily of hydrodynamic origin. The focus of Sec. 4 is primarily on transport in turbulent plasmas, including the diffusion of stochastic magnetic field lines and charged particles, whereas in Sec. 6 we encounter an electrostatic potential advected by an abstract (nonphysical) flow, a problem arising when the effective conductivity of inhomogeneous media (polycrystals, for example) in a strong magnetic field is calculated.

The value of available results on critical behaviors is grossly increased by the *universality of critical exponents* describing the behavior of the order parameter and of other physical quantities near the critical point. Universality implies that the set of critical exponents is structurally stable—that is, it does not change under a small perturbation of the model itself, provided that the perturbation does not introduce long correlations that decay slower than a certain algebraic function. This universality leads to the possibility of new applications of critical phenomena theory that might go far beyond the phase transition problems in statistical physics. Percolation theory has been indeed one of the most interdisciplinary physical models ever introduced.

After a brief introduction to the percolation model and establishing notation (Sec. 2) we focus on various physical applications of percolation theory and statistical topography, such as the advection-diffusion transport of a passive tracer in an incompressible random flow (Sec. 3), enhanced diffusion of particles and heat in turbulent plasmas (Sec. 4), the quantum Hall effect (Sec. 5), and the effective transport coefficients in heterogeneous media (Sec. 6). Some parts of this paper are along the lines of a recent review paper [4]; however, the focus is made on the latest developments and topics not sufficiently

covered in the previous work, such as the quantum Hall effect and the Dykhne method of reciprocal media.

2. Percolation theory and statistical topography

Percolation theory studies the statistics of clusters, viz. connected aggregates, of random geometrical objects. There exist several formulations of the percolation problem both on a lattice and in the continuum.

2.1. Lattice percolation

One of the simplest, *bond percolation problem* is formulated as follows. Consider a lattice network, whose bonds are "conducting" with the probability of p (independent of each other) and hence "blocked" with the probability $1-p$. The clusters of connected conducting bonds determine the "conducting grains." For the probability above a *percolation threshold*, $p > p_c$, the conducting grains join into an *infinite cluster* meaning the transition to a conducting "phase" (Figure 1).

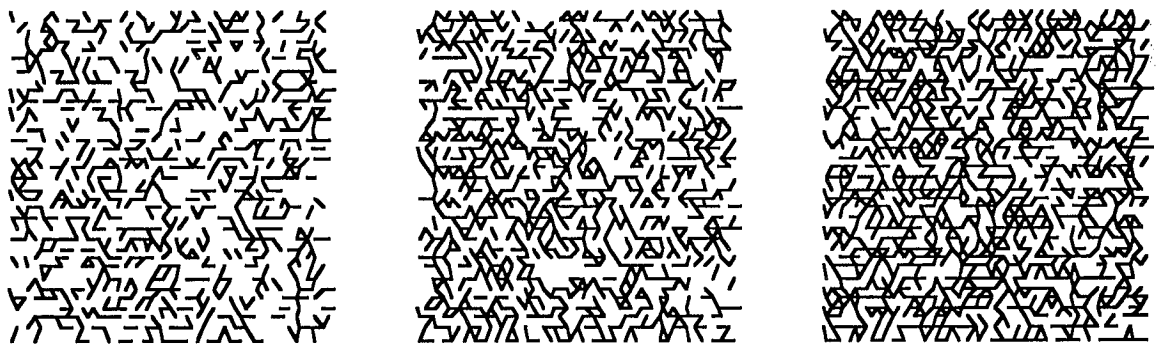

Figure 1: Bond percolation on a triangular lattice. At the critical probability $p_c = 2\sin(\pi/18) \simeq 0.3473$ an infinite cluster first appears and persists at $p > p_c$.

The lattice formulation of the percolation problem was used to describe the hopping conduction in semiconductors (Shklovskii and Efros, 1984) and is quite a popular model in phase transition theory.

Slightly below the percolation threshold p_c, that is, for $0 < p_c - p \ll 1$, all clusters are finite, with the maximum attainable size,[1] or the cluster correlation length, given by the diverging expression

$$\xi(p) \approx \lambda_0 |p - p_c|^{-\nu} , \tag{5}$$

where λ_0 is the lattice cell size. In two dimensions, the correlation length exponent ν is known exactly: $\nu = 4/3$ (cf. [4] and references therein). The three-dimensional

[1]To be more precise, the size separating algebraically scarce clusters from exponentially scarce clusters.

correlation-length exponent is known only from numerics, $\nu \simeq 0.9$. For $p > p_c$, the length (5) describes the maximum size of "holes" in the infinite cluster (or, equivalently, the maximum size of the clusters made of blocked bonds).

Clusters near the percolation threshold are fractals on the length scales $[\lambda_0, \xi]$; the fractal dimension of a cluster is $91/48 \simeq 1.90$ in two dimensions, and approximately 2.5 in three dimensions [10].

To describe conduction and diffusion in disordered media, the model of random (or "vandalized") resistor network has been widely used, where the conducting bonds are assigned unit conductance and the blocked bonds are assigned zero conductance. Then the long-range conductivity σ^* of the system is clearly zero below the percolation threshold, but finite above the threshold:

$$\sigma^*(p) \propto |p - p_c|^{\mu} \theta(p - p_c) \ , \quad |p - p_c| \ll 1 \ , \tag{6}$$

where μ is the percolation conductivity exponent. Like other lattice percolation exponents, μ depends only on the dimensionality of the problem. In two dimensions $\mu \simeq 1.2$, in three dimensions $\mu \simeq 1.7$. These are numerically computed values. So far, no one was able to determine μ analytically. The effective conductivity (6) is a self-averaged quantity only for sufficiently large samples, namely with the size much greater than the correlation, or the mixing scale (5). For smaller samples the effective conductivity will exhibit a power-law size effect.

Another geometrical object associated with a percolation cluster is the cluster perimeter, or the "hull," which is a line enveloping the cluster from either outside or from an inside hole (Figure 2).

For a large two-dimensional percolation cluster with the linear size $a \gg \lambda_0$, the hull is a fractal curve with the fractal dimension of $d_h = 7/4$ [11], hence the hull perimeter L scales with its diameter a as

$$L(a) \approx \lambda_0 (a/\lambda_0)^{d_h} \ , \quad a \gg \lambda_0 \ . \tag{7}$$

The critical probability p_c depends on the kind of lattice. The critical exponents ν, d_h, μ, etc., are empirically known to be universal. The universality of critical behavior implies that the critical exponents depend only on the dimension of the space but not on the kind of lattice. Although the exact values $\nu = 4/3$ and $d_h = 7/4$ were actually derived for particular 2D lattices, the same exponents, within a rather good accuracy, were reported numerically for different lattices including irregular ones so that there are pretty good reasons to believe in the exact universality.

2.2. Continuum percolation

An extension of the percolation model to continuum is the problem of contour lines of a random potential $\psi(x, y)$. The statistics of the regions $\psi(x, y) < h = \text{const}$ are described by continuum percolation, which is very similar to lattice percolation. One can imagine the region $\psi(x, y) < h$ (for which the contour lines of ψ are perimeters) as the "flooded area" on a hilly landscape $z = \psi(x, y)$, where h is the water level. Let us identify the mountains (maxima), the valleys (minima), and the mountain passes (saddle points) of $\psi(x, y)$, as shown in Figure 3.

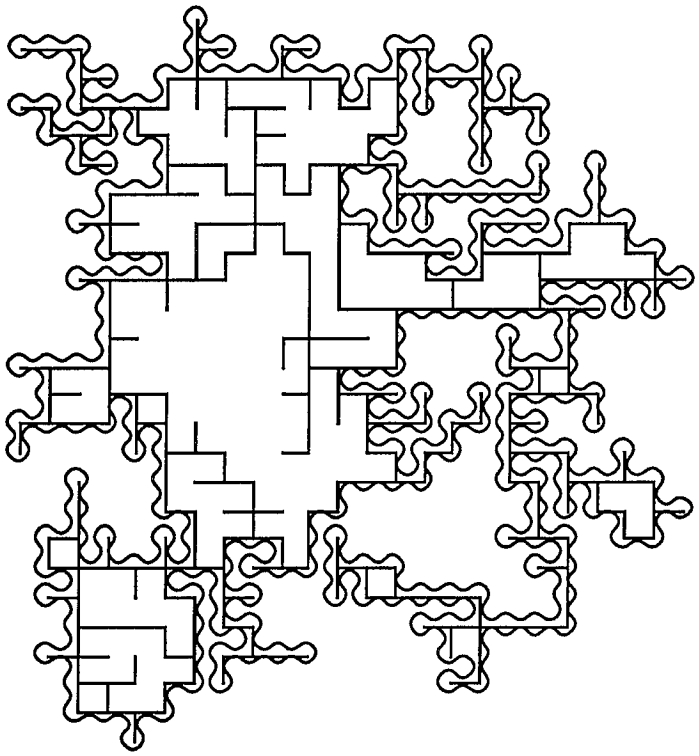

Figure 2: The external hull of a bond cluster on a square lattice.

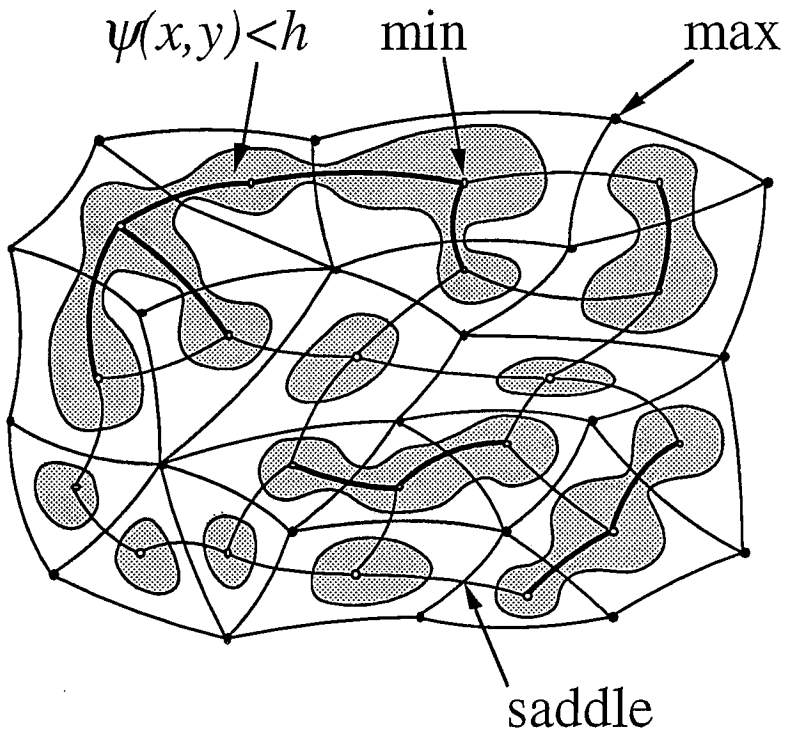

Figure 3: The equivalent lattice of a random potential. Full circles are the maxima and the empty circles are the minima. The steepest descent lines cross at the saddle points.

Then two lakes in the neighboring valleys are connected if the water level is higher than the corresponding saddle point elevation: $\psi_s < h$. Let us designate a steepest descent line, connecting two neighboring minima and coming through the saddle, as a bond. The bond is said to be "conducting" if $\psi_s < h$. As the potential is random, we can introduce the probability of the bond conductance,

$$p(h) = \int_{-\infty}^{h} P(\psi_s) d\psi_s \ , \tag{8}$$

where $P(\psi_s)$ is the probability distribution function of the saddle heights. Thus we infer that the flooded regions are similar to the bond-clusters on the equivalent network generated by the minima and the saddles of ψ. Then the contours of constant ψ are the perimeters of the percolation clusters. Due to the universality of critical behavior, the exponents of the lattice and the continuum percolation must be the same.

The only trouble to worry about is the assumption of the independence of the bond probabilities (8). For a smooth random function, this assumption is generally wrong, since there is always a non-zero covariance $C(\mathbf{x} - \mathbf{x}') = \langle \psi(\mathbf{x}) \psi(\mathbf{x}') \rangle$. However, the critical universality extends further to the case of moderately correlated percolation and holds for sufficiently fast decaying covariance [12,13],

$$C(r) = O(r^{-2/\nu}) = O(r^{-3/2}) \ , \quad \text{for} \quad r \gg \lambda_0 \ . \tag{9}$$

Below this is assumed to be the case, specifying the "monoscale" approximation for the random potential $\psi(\mathbf{x})$.

Upon establishing the correspondence between the contour lines of ψ and the hulls of percolation clusters, we can introduce the critical level $h = h_c$, near which the maximum contour size ξ diverges analogously to expression (5):

$$\xi(h) \approx \lambda_0 \left| \frac{h - h_c}{\psi_0} \right|^{-\nu} \ , \tag{10}$$

where ψ_0 is the variance of $\psi(x, y)$. For a sign-symmetric function $\psi(x, y)$, which is statistically equivalent to $-\psi(x, y)$, the critical level is clearly zero. Expression (7) yields the length of a contour with the linear size a.

Given the characteristic size $a \gg \lambda_0$ of contours we are interested in, the characteristic range of the level values h, at which these contours may be located, is found from Eq. (10):

$$|h - h_c| \leq \psi_0 (\xi / \lambda_0)^{-1/\nu} \ , \tag{11}$$

otherwise the occurence of such contours would be exponentially improbable. Since the characteristic gradient of ψ is known, $|\nabla \psi| \approx \psi_0 / \lambda_0$, Eq. (11) yields the width of a cell formed by the isolines with the size of order a,

$$w(a) \approx \lambda_0 (a / \lambda_0)^{-1/\nu} \ . \tag{12}$$

The results (7), (10), and (12) specify the statistical topography of a monoscale (short-correlated) random relief. For the random flow (1), the connected bundles of contours with similar size play the role of convection cells (Figure 4).

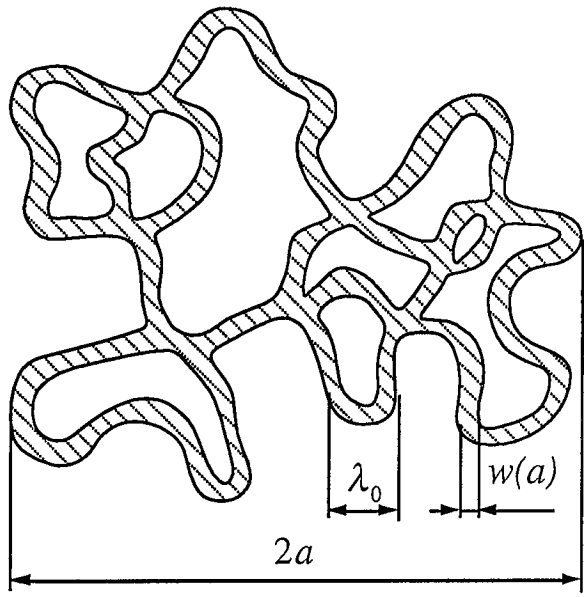

Figure 4: Convection cell in a random velocity field.

There exist a fundamental difference between percolation in two and in higher dimensions. On a two-dimensional isotropic flooded relief, one cannot go to infinity both by sea and by land simultaneously. Hence the percolation level h_c is unique; it corresponds to the open coastline which appears at the sharp moment when, as the water level goes up, the last land path to infinity disapears and the first sea path to infinity is conceived. To the contrast, the topology of three dimensions assumes the possibility of simultaneously percolating "3D land" and "3D ocean," hence there exist two critical levels h_{1c} and h_{2c} so that at $h < h_{c1}$ or at $h > h_{c2}$ only dry or wet (respectively) regions stretch to infinity, whereas at $h_{c1} < h < h_{c2}$ there is percolation through both wet and dry.

3. Diffusion in two-dimensional random, steady flows

Most truly or approximately two-dimensional systems encountered in nature are such due to either a strong magnetic field (plasma) or a fast rotation (large-scale ocean and atmospheric motions). Any two-dimensional incompressible flow can be written in the form (1) and therefore has regular (integrable) streamlines, namely the (closed) contours of the stream function $\psi(x, y)$. Hence without molecular diffusion there will be no effective diffusion. At a small but finite melecular diffusivity D_0, the behavior of the effective diffusivity D^* in the large-Péclet-number limit will depend on the topology of the streamlines. The geometry of 2D random flows assumes the presence of arbitrarily large streamlines, although their share falls off with the increasing size. To estimate the effective diffusivity in such a flow, statistical topography of the stream function must be used [14—16].

It is weird to imagine a time-independent, or a slowly time-dependent, 2D random flow in such traditional 2D hydrodynamic objects as atmosphere or ocean where the characteristic frequency ω is typically of the order of the inverse eddy rotation time, $\omega \simeq$

v_0/λ_0. The practical implications of "frozen," or "quenched" 2D random flows involve primarily condensed-matter objects, such as quantum diffusion [17], the quantum Hall effect [18] inhomogeneously doped semiconductors [19,20] or plasma openning switches [21,22]. The case of a slowly varying flow, $\omega \ll v_0/\lambda_0$, is also encountered in the problem of diffusion in turbulent plasmas (Sec. 4).

For a monoscale stream function $\psi(x,y)$ heuristic arguments can be used to derive the scaling

$$D^* \simeq D_0 \left(\frac{\psi_0}{D_0}\right)^{\alpha}, \quad \psi_0 \equiv \psi_{\rm rms} \gg D_0 \ , \tag{13}$$

where the exponent is expressed through the 2D percolation indices $\nu = 4/3$ and $d_h = 7/4$:

$$\alpha = \frac{\nu d_h + 1}{\nu d_h + 2} = \frac{10}{13} \ . \tag{14}$$

The derivation of result (13) employs a "hypothesis of broken coherence." This hypothesis assumes that particle displacements may be considered essentially uncorrelated if the streamlines on which these displacements are experienced differ twice or more in size. In this way, one naturally comes to the concept of a convection cell being the conglomerate of streamlines with diameter between a and $2a$ (Figure 4). The mixing length ξ_m is then determined as the size of convection cells producing the most efficient coherent contribution to transport. The estimate is quite similar to the standard boundary-layer argument used for regular convection patterns (cf. [23]). The difference, however, is that the convection cells in a random flow are diverse, and their size a, width $w(a)$, and perimeter $L(a)$ are coupled in a fashion determined by the statistics of the random field $\psi(x,y)$. For example, for a monoscale (λ_0) flow the relations given by Eqs. (7) and (12) should be used. The mixing length ξ_m is defined as the cell size where the convection time equals the transverse diffusion time,

$$\frac{L(\xi_m)}{v_0} = \frac{w^2(\xi_m)}{D_0} \ , \tag{15}$$

where $v_0 = \psi_0/\lambda_0$ is the characteristic velocity. Substituting expressions (7) and (12) for the length $L(a)$ and the width $w(a)$ of the convection cell, we find

$$\xi_m = \lambda_0 \, P^{\frac{\nu}{\nu d_h + 2}} \ , \quad P \equiv \frac{\psi_0}{D_0} \gg 1 \ . \tag{16}$$

The effective diffusivity is then estimated to be

$$D^* \simeq F(\xi_m) \frac{\xi_m^2}{w^2(\xi_m)/D_0} = v_0 \, w(\xi_m) \ , \tag{17}$$

where $F(a) = L(a)w(a)/a^2 \simeq \lambda_0/a$ is the fraction of area covered by the convection cells of a specified size. Upon substituting expression (16) into (17) we arrive at the result (13).

The percolation scaling of the effective diffusivity involving the exponent $\alpha = 10/13$ appears to be as universal as the static exponents of continuum percolation. This implies

that the randomness (in the sense of the ensemble averaging) of the velocity field is not really necessary for the result (13) to be valid; the *genericity*, i.e., the absence of exceptional features like periodicity, etc., may be sufficient. Yet, the presence of long-range correlations even in a random the velocity field can significantly modify the scaling of the effective diffusivity [14,24].

The computation of the effective diffusivity for high-order quasi-periodic flows, having extended streamlines, showed a very good agreement with the "10/13" scaling [25] In general, the direct particle simulation of effective diffusion at large Péclet number is extremely expensive because the integration accuracy must be good enough to spatially resolve the narrow boundary layers and not to overlook the long-range ($\xi_m \gg \lambda_0$) correlations in the particle orbits. The success of Chernikov and Rogalsky [25] lies in the trick borrowed from the theory of Hamiltonian chaos, whereby the actual orbit integration is replaced by a large-step mapping on a stochastic web, which is an exponentialy thin envelope of exact Hamiltonian contours.

4. Turbulent transport in plasmas

The anomalous diffusion of particles and heat in fusion plasmas is the major problem of controlled fusion due to the presence of poorly controllable turbulent collective fluctuations in a tokamak. These fluctuations act like additional scattering centers leading to a substantial enhancement of diffusion as compared to the (never attainable) case of a quiescent plasma. A strong magnetic field $\mathbf{B}$ does suppress the turbulent diffusion, but to a lower extent compared with the standard Coulomb-scattering (quiescent) scaling $D^* \propto B^{-2}$.

Mathematically, the turbulent transport in a plasma can be often described by the advection of an agent, such as temperature, in a random incompressible flow. Although this advection is usually not quite passive (for example, the temperature gradient can drive the self-consistent plasma turbulence), the idea of universality suggests that the scalings of turbulent transport can be analytically predicted based on the very approximate knowledge as to what class of universality we are in. Experimental data on tokamaks often indicate the presense of a well defined length scale of the turbulence, with apparently no long-range correlations in the velocity field. Analogously to correlations in the flow, one can expect that the percolational universality of the effective diffusion also survives a moderate feedback between the advected agent and the advecting flow. Hence the percolation-theory based estimates of the turbulent transport may be not a bad approximation to what really happens.

Turbulent difusion in plasmas is a problem different from the one discussed in Sec. 3 in that the collisional diffusivity is usually negligible in comparison with the effects of the time-dependence of the flow. Hence, instead of the Péclet number, another nondimensional parameter is relevant, namely the Kubo number

$$K = \frac{v_0}{\lambda_0 \omega} , \tag{18}$$

where ω is the characteristic frequency of the evolution of the flow. Unlike the case of neutral fluids, where nonlinear dynamics usually impose $K \simeq 1$, the Kubo number in plasma turbulence can, in principle, vary in a wide range.

The guiding center motion of a charged particle in crossed electric [$\mathbf{E} = -\nabla\phi(\mathbf{x}, t)$] and magnetic ($\mathbf{B} = B_0\,\hat{\mathbf{z}}$) fields is described by

$$\frac{d\mathbf{x}}{dt} = v_\parallel\,\hat{\mathbf{z}} + c\,\frac{\mathbf{E}\times\mathbf{B}}{B^2}\ , \tag{19}$$

which corresponds to an incompressible motion across the magnetic field with the stream function

$$\psi(x,y,t) = -\frac{c}{B_0}\,\phi\left(x, y, z_0 + \int_0^t v_\parallel(t')dt', t\right)\ . \tag{20}$$

The characteristic frequency $\omega = \max(\omega_*, k_\parallel v_\parallel)$ (where $\omega_* \simeq |\partial \log\phi/\partial t|$) and $k_\parallel \simeq |\partial\log\phi/\partial z|$), may be decoupled from the amplitude of ψ. This leads to the possibility of both the high-frequency regime $K \ll 1$, also known as the *quasilinear* limit, and the low-frequency ($K \gg 1$), or the *percolation* regime of turbulent diffusion (Isichenko and Horton, 1991).

Another example is plasma heat conduction in a magnetic field with a small random component, $\mathbf{B} = B_0\,\hat{\mathbf{z}} + \delta\mathbf{B}_\perp(\mathbf{x})$, $\delta\mathbf{B}_\perp = \nabla A_\parallel(\mathbf{x})\times\hat{\mathbf{z}}$. The equation of a magnetic field line in the form

$$\frac{d\mathbf{x}_\perp}{dz} = \frac{\delta\mathbf{B}_\perp}{B_0} \tag{21}$$

is equivalent to the incompressible advection with the stream function $\psi(\mathbf{x}_\perp, z) = A_\parallel(\mathbf{x}_\perp, z)/B_0$ and the coordinate z standing for time. The turbulent diffusivity stemming from Eq. (21) is known as the magnetic field line diffusivity D_m [27]. This quantity has the dimensionality of length. In a collisionless plasma, the diffusive walk of magnetic lines causes an enhanced electron thermal conductivity across the background magnetic field [28—30],

$$D_\perp^* \simeq D_m\,v_e\ , \tag{22}$$

where v_e is the thermal velocity of electrons moving along the magnetic field lines.

The above examples motivated the study of turbulent diffusion in two dimensions, with the characteristic flow frequency ω considered a free parameter. In the quasilinear limit $\omega \gg v_0/\lambda_0$, the effective diffusivity is insensitive to the topology of streamlines because the flow is unrecognizably changed in the short correlation time of ω^{-1} — that is, well before a tracer particle is displaced by the distance λ_0. The particle displacement in the correlation time is of order v_0/ω leading to the turbulent diffusivity

$$D^* \simeq \frac{v_0^2}{\omega} = \lambda_0^2\omega K^2\ , \quad K \ll 1\ . \tag{23}$$

In the opposite, low-frequency limit $\omega \ll v_0/\lambda_0$, a tracer particle can move along an almost steady streamline to a large distance before the flow pattern has changed appreciably.

Consider a monoscale, random, slowly varying, two-dimensional flow. The mixing length ξ_m is defined as the maximum coherent particle displacement that occurs in the lifetime $\tau(\xi_m)$ of the convection cell:

$$L(\xi_m) = v_0\,\tau(\xi_m) \tag{24}$$

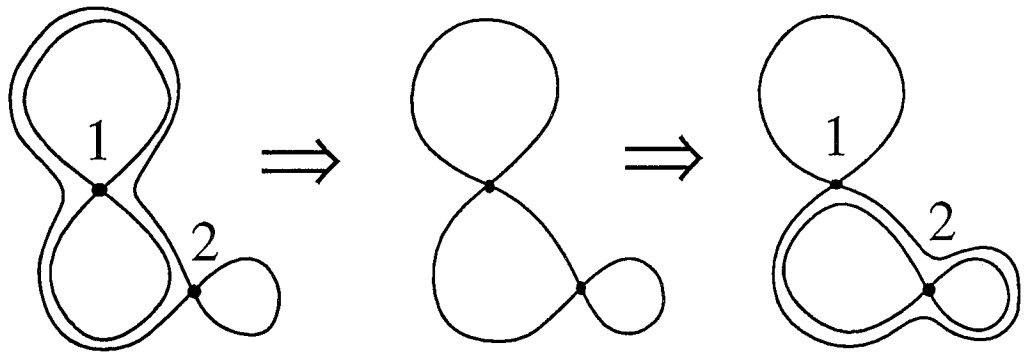

Figure 5: The reconnection of separatrices.

[compare with (15)]. The lifetime $\tau(a)$ of an a-cell is the time of an unrecognizable change in the shape of a contour $\psi(x,y,t) = h$ with the initial diameter a. Such a change is undergone through the contour reconnection process (Figure 5). The reconnection takes place when the saddles corresponding to neighboring separatrices come through the same level. An essential change in the shape of the convection cell occurs when the saddles pass the level difference $\delta\psi = \psi_0 w(a)/\lambda_0$ corresponding to the width of the cell $w(a)$ given by Eq. (12). As the level of a saddle point changes at the characteristic rate $\psi_0\omega$, the lifetime of the convection cell is estimated to be

$$\tau(a) = \frac{\delta\psi}{\psi_0\omega} = \frac{w(a)}{\lambda_0\,\omega}\ . \tag{25}$$

Upon substituting Eq. (25) into (24), we find the mixing scale

$$\xi_m = \lambda_0 K^{\frac{\nu}{\nu d_h+1}}\ . \tag{26}$$

The turbulent diffusivity is then estimated similarly to (17),

$$D^* \simeq F(\xi_m)\,\frac{\xi_m^2}{\tau(\xi_m)} = v_0\,w(\xi_m) = \lambda_0^2\omega K^{7/10}\ , \quad K \gg 1\ . \tag{27}$$

A positive feature of the percolation scaling (27) is that it predicts a much slower growth of the turbulent diffusivity with the turbulence amplitude K, as compared with the usually used quasilinear estimate (23) and even the "renormalized" strong turbulence scaling $D^* \propto K$, which may be too pessimistic. This is especially nice since the self-consistent plasma turbulence is not yet well understood and experimentally controlled.

5. The quantum Hall effect

We now downscale from the thermonuclear temperatures of order 10^8 Kelvin to the liquid helium temperatures of order 1 Kelvin, where the quantization of Hall conductance can be observed [31,32]. One then deals with another kind of plasma, namely the two-dimensional electron gas, created by freezing out the third degree of freedom to the ground state in a gap voltage applied to a semiconductor inversion layer. The essence

of the quantum Hall effect (QHE) is that the measured conductivity tensor of the 2D electron gas at low temperature is

$$\hat{\sigma} = \begin{pmatrix} 0 & -Ne^2/h \\ Ne^2/h & 0 \end{pmatrix}, \tag{28}$$

where e is the electron charge, h the Planck constant and N an integer, with an accuracy of several parts in ten million, thereby having important implications in metrology. The diagram of measured Hall and Ohmic conductances is presented in Figure 6.

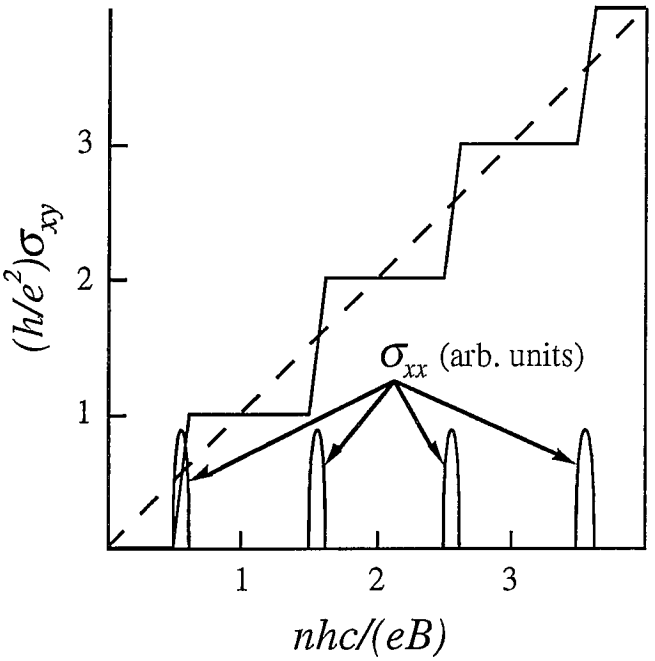

Figure 6: The schematic dependence of Hall and Ohmic conductivities on the magnetic field in the regime of quantum Hall effect. The dashed line shows the classical behavior of σ_{xy} [Eq. (30)].

An interesting thing is that the presence of impurities is not only harmless (up to a certain point) but even necessary for the high-precision QHE. As we will see, the role of disorder in the QHE is also conected with percolation.

The described above integer QHE can be well understood on the basis of an elementary model of a 2D gas of noninteracting electrons [33]. As the normalization of Fig. 6 shows, the integer N in Eq. (28) is the number of filled Landau energy levels, $E_j = \hbar\omega_c(j + 1/2)$, where $\omega_c = eB/(mc)$ is the cyclotron frequency. In a translationally uniform system, each Landau level is multiply degenerate, the number of degenerate states per unit area being

$$n_B = \frac{1}{2\pi l^2} = \frac{eB}{hc}, \tag{29}$$

where $l = \sqrt{\hbar c/(eB)}$ is the so-called magnetic length, or the characteristic length of the electron wave function. The degeneracy is lifted by the electrostatic potential $\phi(x, y)$ created by impurities, which broadens the discrete Landau levels into a continuous density of states about each Landau level (Figure 7).

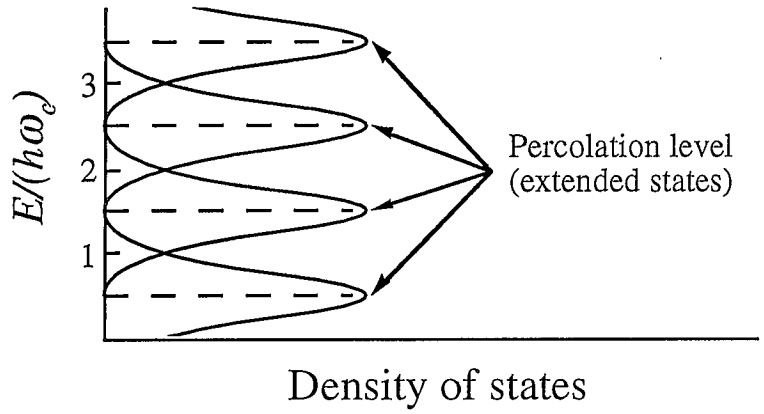

Figure 7: The energy spectrum of the two-dimensional electron gas in a magnetic field.

The new, perturbed states are all localized in the l-vicinities of the corresponding contours of the impurity potential $\phi(x, y)$ [18]. In terms of classical physics, electrons perform the $\mathbf{E} \times \mathbf{B}$ drift motion with exponentially well, or even perpetually conserved adiabatic invariant—the value of the potential at the guiding center. The quantum counterpart of the classical adiabaticity is the stationarity of the orbital quantum number.

The magnetic length l is nothing but the Larmor radius determined at the ground state "temperuature" $T = \hbar\omega_c/2$. If the magnetic length l is much smaller than the characteristic correlation scale λ_0 of the impurity potential ϕ, the localization near a closed contour implies an absolute localization. In two dimensions, however, there exists a sharp critical level $\phi(x, y) = h_c$, where an open isopotential percolates to infinity. Only at this level there do exist extended electron states (Figure 7).

The specific of the Landau quantization is that each filled Landau level suffers an identical broadening in energy over approximately the variance ϕ_0 of the impurity potential. In this sense, the diagram in Figure 7 can be interpreted as the superposition of $N = [n/n_B]$ identical classical electron gases with the density of n_B each, corresponding to fully filled Landau levels, plus a partially filled broadened Landau level.

In the classical collisionless electron gas the conductance is governed by the $\mathbf{E} \times \mathbf{B}$ current $\mathbf{j} = -enc\mathbf{E} \times \mathbf{B}/B^2$, which yields the zero Ohmic conductivity σ_{xx} and the Hall conductivity

$$\sigma_{xy}^{\mathrm{cl}} = -\frac{ecn}{B}\,, \tag{30}$$

where n is the total density of electrons. This contrasts with the quantum expression (28), which can be written using notation (29) as

$$\sigma_{xy}^{\mathrm{qu}} = -\frac{ecNn_B}{B}\,, \tag{31}$$

The crucial point for understanding the QHE is that only extended states can carry electrical current. Hence, as the density n of electrons is increased, the conducting properties of the electron gas are not changed unless the Fermi level crosses the Nth

percolation level on Figure 7. Hence the quantum formula (31) can be interpreted as the classical formula (30), where n is not the density of all electrons but rather the total density of electrons in the Landau levels filled above their respective percolation thresholds. This explains the nature of the integer plateaus on the Hall conductance, as well as the steps at the points where the Fermi level crosses the percolation levels.

As the conductance far from the steps is produced by electrons far from the Fermi level, inelastic scattering process are improbable in proportion to the thermal activation factor $\exp(-\Delta\mathcal{E}/T)$, where $\Delta\mathcal{E}$ is the gap between the percolation and the Fermi levels, and the Ohmic (dissipative) resistivity and conductivity are both zero, as indicated by Eq. (28). In fact, this is the virtually zero diagonal conductivity which makes it possible to measure the Hall conductivity with such a fantastic precision [34,35]. At the steps, the inelastic scattering of electrons is no longer exponentially small, resulting in narrow peaks of the measured Ohmic conductivity (Figure 6).

The width of the steps on the quantized conductance is primarily due to finite temperature. However, even at zero temperature the steps on the quantum Hall conductance have finite width associated with nonlinear effects [18]. In fact, the electric field in a QHE sample consists of the zero-average impurity field $\mathbf{E}_0 = -\nabla\phi(x,y)$ and the externally applied electric field $\mathbf{E}_1 \ll \mathbf{E}_0$. The contour lines of the resulting potential include not only closed lines, like as described in Sec. 2, but also a network of channels filled by open isopotentials. The topography of such a potential is described in terms of "graded percolation," where the local probability p of the bond conductance is a slow function of position. The percolation threshold is thus nonlinearly broadened in the small parameter of E_1/E_0 [18,4].

Thus the integer QHE is due to (a) the discreteness of electron Landau levels in a magnetic field and (b) the two-dimensional nature of the electron gas in an inversion layer so that each impurity-potential-broadened Landau levels has a unique percolation threshold. In three dimensions, this kind of Hall conductance quantization is impossible.

In addition to the integer QHE, there has been also discovered the fractional QHE, where the factor N in (28) takes on fractional values with a small odd denominator [36]. The explanation of the fractional QHE necessarily involves the electron-electron interaction, quasi-particles, and the like. That is, here one deals with a 2D electron fluid rather than a gas [33].

6. Conductivity of inhomogeneous media

The problem of averaging space-varying transport coefficients has been posed frequently, starting from Maxwell (1873). Its general formulation is as follows. Let $\mathbf{e}(\mathbf{x})$ be the microscopic electric field and $\mathbf{j}(\mathbf{x})$ the microscopic current density in a medium with a nonuniform conductivity tensor $\widehat{\sigma}(\mathbf{x})$:

$$\mathbf{j}(\mathbf{x}) = \widehat{\sigma}(\mathbf{x})\,\mathbf{e}(\mathbf{x})\ . \tag{32}$$

To satisfy the time-independent Maxwell's equations, the electric field should be irrotational and the current density solenoidal:

$$\nabla \times \mathbf{e} = 0\ , \qquad \nabla \cdot \mathbf{j} = 0\ . \tag{33}$$

The effective conductivity $\widehat{\sigma}^*$ of the medium is to be calculated.

By definition, the effective conductivity is the tensor describing the relation between the average electric field $\mathbf{E} = \langle \mathbf{e}(\mathbf{x}) \rangle$ and the average current density $\mathbf{J} = \langle \mathbf{j}(\mathbf{x}) \rangle$:

$$\mathbf{J} = \widehat{\sigma}^*[\widehat{\sigma}(\mathbf{x})]\,\mathbf{E}\ , \tag{34}$$

where the square brackets indicate a functional. Analogously to the advection-diffusion problem, one can introduce the mixing length ξ_m characterizing the minimum scale over which the averaging leading to Eq. (34) is to be performed.

In an unmagnetized medium, where the local conductivity tensor is symmetric, $\sigma_{ij}(\mathbf{x}) = \sigma_{ji}(\mathbf{x})$, the electrical current is distributed so that the Ohmic dissipation $\int \mathbf{j}\cdot\mathbf{e}\, d\mathbf{x}$ is a minimum. This variational principle can be used to obtain various bounds on the effective conductivity. For an isotropic unmagnetized medium with $\sigma_{ij}(\mathbf{x}) = \sigma(\mathbf{x})\,\delta_{ij}$ one has (cf. [37])

$$\frac{1}{\langle 1/\sigma \rangle} \le \sigma^* \le \langle \sigma \rangle\ , \tag{35}$$

where the limiting values of σ^* are attained for layered inhomogeneities corresponding to the series and the parallel connection of uniform pieces of the medium, respectively. In a magnetic medium with an antisymmetric (Hall) conductivity component the variational principle is less trivial [20].

If the conductivity contrast is very high [the left-hand side of Eq. (35) is much smaller than the right-hand side], quite nontrivial scalings of σ^* can be expected. One example is given by formula (6) describing the conductivity of a conductor-dielectric mixture *near* the percolation threshold. Below we review in some detail a method of the exact calculation of $\widehat{\sigma}^*$ for a two-pase, two-dimensional mixture *exactly at* the percolation threshold.

6.1. The method of reciprocal media

This method was originally proposed by Keller [38] and independently by Dykhne [39], whose approach appears more elegant and admits easier generalizations. One starts with the Ohm's law (32) where all vectors and space dependences are strictly two-dimensional. Following Dykhne, consider new vector fields

$$\mathbf{j}'(\mathbf{x}) = a\,\widehat{\delta}\,\mathbf{j}(\mathbf{x}) - b\,\widehat{\epsilon}\,\mathbf{e}(\mathbf{x})\ , \qquad \mathbf{e}'(\mathbf{x}) = c\,\widehat{\delta}\,\mathbf{e}(\mathbf{x}) - d\,\widehat{\epsilon}\,\mathbf{j}(\mathbf{x})\ , \tag{36}$$

where $\widehat{\delta} = \delta_{ik}$ is the Kronneker tensor, $\widehat{\epsilon} = \epsilon_{ik}$ the Levi-Cività tensor (rotation through 90^0), and $a, \ldots, d$ arbitrary constants. The choice of $\mathbf{j}'$ and $\mathbf{e}'$ is designed to satisfy the relations

$$\nabla\cdot\mathbf{j}' = 0\ , \qquad \nabla\times\mathbf{e}' = 0 \tag{37}$$

that follow from (33) and (36). (This trick only works in two dimensions.) Upon comparing the Ohm's law (32) with Eqs. (36) one easily finds the relation between the "primed" vector fields,

$$\mathbf{j}'(\mathbf{x}) = \widehat{\sigma}'(\mathbf{x})\,\mathbf{e}'(\mathbf{x})\ , \tag{38}$$

where

$$\widehat{\sigma}'(\mathbf{x}) = \left(a\,\widehat{\delta} + d\,\widehat{\sigma}(\mathbf{x})\,\widehat{\epsilon}\right)^{-1}\left(b\,\widehat{\epsilon} + c\,\widehat{\sigma}(\mathbf{x})\right)\ . \tag{39}$$

Once it is assumed that from (32) and (33) the relation (34) follows, we conclude that in quite the same way from (37) and (38) the following effective Ohm's law for the primed system also holds:

$$\mathbf{J}' = \widehat{\sigma}^*[\widehat{\sigma}'(\mathbf{x})]\,\mathbf{E}' \ , \tag{40}$$

where $\widehat{\sigma}^*[\ldots]$ denotes *the same* functional as in Eq. (34). As the averaged electric field and current of the new system are related to the average fields of the old system identically to the relation between the microscopic fields [Eq. (36)], we can formulate the general *reciprocity theorem* as follows:

$$\widehat{\sigma}^*\left[\left(a\,\widehat{\delta} + d\,\widehat{\sigma}(\mathbf{x})\,\widehat{\epsilon}\right)^{-1}\left(b\,\widehat{\epsilon} + c\,\widehat{\sigma}(\mathbf{x})\right)\right] = \left(a\,\widehat{\delta} + d\,\widehat{\sigma}^*[\widehat{\sigma}(\mathbf{x})]\,\widehat{\epsilon}\right)^{-1}\left(b\,\widehat{\epsilon} + c\,\widehat{\sigma}^*[\widehat{\sigma}(\mathbf{x})]\right) \ . \tag{41}$$

In the particular case of an isotropic 2D medium, the microscopic conductivity tensor can be written as

$$\widehat{\sigma}(\mathbf{x}) = \begin{pmatrix} D & \psi \\ -\psi & D \end{pmatrix} = D(x,y)\,\widehat{\delta} + \psi(x,y)\,\widehat{\epsilon} \ . \tag{42}$$

Then the reciprocity relation (41) states that the components of the effective conductivity tensor satisfy

$$D^*[D',\psi'] = \frac{(ac+bd)D^*[D,\psi]}{(a-d\psi^*[D,\psi])^2 + (dD^*[D,\psi])^2} \ , \tag{43}$$

$$\psi^*[D',\psi'] = \frac{ab + (ac-bd)\psi^*[D,\psi] - cd(\psi^{*2}[D,\psi]) + D^{*2}[D,\psi])}{(a-d\psi^*[D,\psi])^2 + (dD^*[D,\psi])^2} \ , \tag{44}$$

where

$$D' = \frac{(ac+bd)D}{(a-d\psi)^2 + (dD)^2} \ , \tag{45}$$

$$\psi' = \frac{ab + (ac-bd)\psi - cd(\psi^2 + D^2)}{(a-d\psi)^2 + (dD)^2} \tag{46}$$

are the microscopic parameters of the second (reciprocal) system.

Formulas (41) and (43)–(46) connect the efective conductivities of two different inhomogeneous media. Some useful corrolaries are obtained when the arbitrary constants $a,\ldots,d$ are appropriately chosen.

6.2. Two-phase systems

Now consider a system consisting of only two phases, I and II, where $D(\mathbf{x})$ and $\psi(\mathbf{x})$ take on the values, D_1 and D_2, and ψ_1 and ψ_2, respectively. In order to get a closed system of equations sufficient for the calculation of the effective conductivity tensor, we wish to choose the constants $a,\ldots,d$ such that the new medium (and hence its effective conductivity) is simply related to the old system.

6.2.1. Equivalently distributed phases

are amenable to a complete analytical solution, because it is possible to choose a, b, c, d such that the new medium (45)–(46) differs from the old one by only the interchange of the phases, and hence is equivalent to the old system. So we are solving the system of four equations,

$$D_i' \equiv \frac{(ac+bd)D_i}{(a-d\psi_i)^2+(dD_i)^2} = D_j \ , \tag{47}$$

$$\psi_i' \equiv \frac{ab+(ac-bd)\psi_i - cd(\psi_i^2+D_i^2)}{(a-d\psi_i)^2+(dD_i)^2} = \psi_j \ , \tag{48}$$

where $i = 1,2$ and $j = 3-i$. With no harm to generality we put $a = 1$ and find

$$b = 2\,\frac{\Delta_1 D_2 - \Delta_2 D_1}{\psi_1 D_2 - \psi_2 D_1} \ , \tag{49}$$

$$c = -1 \ , \tag{50}$$

$$d = 2\,\frac{D_1 + D_2}{\psi_1 D_2 - \psi_2 D_1} \ , \tag{51}$$

where the notation $\Delta_i = D_i^2 + \psi_i^2$ is introduced for brevity. Then from Eqs. (43)–(44) we find the effective conductivity parameters of an isotropic mixture of two equivalently distributed phases:

$$D_{1/2}^* = \frac{ac+bd-\left(\frac{a+c}{2}\right)^2}{d^2} = \sqrt{D_1 D_2 \left(1+\left(\frac{\psi_1-\psi_2}{D_1+D_2}\right)^2\right)} \ , \tag{52}$$

$$\psi_{1/2}^* = \frac{a-c}{2d} = \frac{\psi_1 D_2 + \psi_2 D_1}{D_1 + D_2} \ , \tag{53}$$

where the subscript "1/2" emphasizes the 50/50 split area occupation by the phases, a necessary (yet not sufficient) condition of the equivalence between the phases.

Results (52)–(53) are equivalent to those obtained by Balagurov [40]. In the limit of an unmagnetized medium, where $\psi_1 = \psi_2 = 0$, formula (52) reduces to the well-known geometric mean of the conductivities of the two equivalently distributed phases [39].

The method of reciprocal media was also used for the electrical conductivity in polycrystals [39], plasma heat conduction in stochastic magnetic fields [29,41], and the magnetoresistance of metals [35].

6.2.2. Non-equivalent phases

If the interchange of the phases does change the system macroscopically, one cannot derive the effective conductivity, even though the concentrations of the phases might be given. Nevertheless, one useful relation between the effective parameters D^* and ψ^* can be obtained without any further assumptions. This is due to the existence of another

reciprocity transformation which amounts to the change of the sign of the magnetic field: $D_i' = D_i$, $\psi_i' = -\psi_i$. Solving these equations for b, c, and d (at $a = 1$) we obtain

$$b = 2\,\frac{\psi_1\Delta_2 - \psi_2\Delta_1}{\Delta_1 - \Delta_2}\ , \tag{54}$$

$$c = 1\ , \tag{55}$$

$$d = 2\,\frac{\psi_1 - \psi_2}{\Delta_1 - \Delta_2}\ . \tag{56}$$

Then Eq. (44) reduces to an identity, whereas Eq. (43) yields the desired relation:

$$(D^*)^2 + (\psi^* - \psi_0)^2 = D_0^2\ , \tag{57}$$

where

$$\psi_0 = \frac{1}{2}\frac{\Delta_1 - \Delta_2}{\psi_1 - \psi_2}\ , \tag{58}$$

$$D_0 = \frac{1}{2}\sqrt{(\psi_1 - \psi_2)^2 + 2(D_1^2 + D_2^2) + \left(\frac{D_1^2 - D_2^2}{\psi_1 - \psi_2}\right)^2}\ . \tag{59}$$

So, if a system consists of only two phases with specified parameters, and only the geometry and the concentration of the phases are arbitrarily changed, the effective conductivity in the plane (D^*, ψ^*) may not be arbitrary but is constrained to lie on the circle (57). An intriguing feature of the fractional quantum Hall effect is that the "circle relation" (57) is actually measured in the steps of the Hall conductance [42].

6.3. Advection-diffusion analogy

A noticeable feature of conducting media with the Hall efect is that the conductivity processes are related to advection-diffusion transport in an incompressible steady flow, which is a problem amenable to a more or less clear qualitative analysis. The correspondence between the two problems [19] follows from the microscopic Ohm's law, $\mathbf{j}(x) = \hat{\sigma}(\mathbf{x})\,\mathbf{e}(\mathbf{x})$, $\mathbf{e}(\mathbf{x}) = -\nabla\phi(\mathbf{x})$, and the requirement that the current density $\mathbf{j}(\mathbf{x})$ be divergence-free:

$$\frac{\partial}{\partial x_i}\,\sigma_{ij}(\mathbf{x})\,\frac{\partial\phi}{\partial x_j} = 0\ . \tag{60}$$

Upon substituting the expression

$$\sigma_{ij}(\mathbf{x}) = \sigma_{ij}^s(\mathbf{x}) + \sigma_{ij}^a(\mathbf{x})\ , \tag{61}$$

where $\sigma_{ij}^s = \sigma_{ji}^s$ and $\sigma_{ij}^a = -\sigma_{ji}^a$, into Eq. (60), we obtain

$$\mathbf{v}\cdot\nabla\phi = \nabla(\hat{\sigma}^s\nabla\phi)\ , \tag{62}$$

where

$$v_i(\mathbf{x}) = \frac{\partial\sigma_{ij}^a(\mathbf{x})}{\partial x_j} \tag{63}$$

is an incompressible ($\boldsymbol{\nabla} \cdot \mathbf{v} = \nabla_i \nabla_j \sigma^a_{ij} \equiv 0$) "velocity" field. Equation (62) can be thought of as describing the steady distribution of a tracer with the density ϕ, advected by the flow $\mathbf{v}(\mathbf{x})$ and subject to the "molecular diffusion" $\widehat{\boldsymbol{\sigma}}^s(\mathbf{x})$. This is this physical analogy which motivated our notation in Eq. (42). Notice that the vector potential $\boldsymbol{\psi}(\mathbf{x})$ of the flow $\mathbf{v}(\mathbf{x})$ is given by

$$\psi_i = \frac{1}{2} \varepsilon_{ijk} \sigma^a_{jk} \ , \qquad \sigma^a_{ij} = \varepsilon_{ijk} \psi_k \ , \tag{64}$$

where ε_{ijk} is the 3D Levi-Cività tensor. For bounded fluctuations in the Hall conductivity $\widehat{\boldsymbol{\sigma}}^a(\mathbf{x})$ the vector potential $\boldsymbol{\psi}(\mathbf{x})$ is also bounded, leading to the existence of a finite effective diffusivity tensor $\widehat{\mathbf{D}}_{\text{eff}}$ [43] In terms of a steady tracer distribution, this means that the average flux be proportional to the average density gradient:

$$\langle \mathbf{v}\phi - \widehat{\boldsymbol{\sigma}}^s \boldsymbol{\nabla}\phi \rangle = -\widehat{\mathbf{D}}_{\text{eff}} \langle \boldsymbol{\nabla}\phi \rangle \ , \tag{65}$$

where the angular brackets denote the spatial average over scales much larger than a certain mixing scale ξ_m. Upon integrating the left-hand side of Eq. (65) by parts, one finds

$$\langle \widehat{\boldsymbol{\sigma}} \boldsymbol{\nabla}\phi \rangle = \widehat{\mathbf{D}}_{\text{eff}} \langle \boldsymbol{\nabla}\phi \rangle + \langle \boldsymbol{\psi} \rangle \times \langle \boldsymbol{\nabla}\phi \rangle \ . \tag{66}$$

Since the left-hand side of Eq. (66) is just the average current density, we recover the average Ohm's law with the effective conductivity tensor (Dreizin and Dykhne, 1972)

$$\widehat{\boldsymbol{\sigma}}^* = \widehat{\mathbf{D}}_{\text{eff}} + \langle \widehat{\boldsymbol{\sigma}}^a(\mathbf{x}) \rangle \ . \tag{67}$$

Thus, if one is able to determine the effective diffusivity $\widehat{\mathbf{D}}_{\text{eff}}$ in the flow (63) with the molecular diffusivity $\widehat{\boldsymbol{\sigma}}^s$, formula (66) yields the exact result for the effective conductivity of the inhomogeneous medium with the Hall effect.

As the effective diffusion $\widehat{\mathbf{D}}_{\text{eff}}$ depends only on the derivatives of $\widehat{\boldsymbol{\sigma}}^a(\mathbf{x})$, it follows from Eq. (67) that the effective conductivity tensor $\widehat{\boldsymbol{\sigma}}^*$ contains a constant addition to $\widehat{\boldsymbol{\sigma}}^a$ also additively. Besides, it also follows that under the change in the sign of the magnetic field [$\widehat{\boldsymbol{\sigma}}^a(\mathbf{x}) \to -\widehat{\boldsymbol{\sigma}}^a(\mathbf{x})$, $\widehat{\boldsymbol{\sigma}}^s(\mathbf{x})$ intact] the simmetric (Ohmic) component $\widehat{\boldsymbol{\sigma}}^{*s}$ of the effective conductivity does not change whereas the Hall component $\widehat{\boldsymbol{\sigma}}^{*a}$ reverses its sign.

In two dimensions, there exist two dual representations of the advection-diffusion analogy. The first is in terms of the electrostatic potential ϕ,

$$-\{\sigma_{xy}, \phi\} = \boldsymbol{\nabla} (\sigma_{xx} \boldsymbol{\nabla}\phi) \ , \tag{68}$$

where the Poisson bracket $\{a, b\} = \boldsymbol{\nabla} a \times \boldsymbol{\nabla} b \cdot \hat{\mathbf{z}}$ describes the advection of b by the flow with the stream function a, $\sigma_{xx} = D(x, y)$, $\sigma_{xy} = \psi(x, y)$.

The second representation is in terms of the stream function h (or the magnetic field) of the electric current $\mathbf{j} = \boldsymbol{\nabla} h \times \hat{\mathbf{z}}$,

$$-\{\rho_{xy}, h\} = \boldsymbol{\nabla} (\rho_{xx} \boldsymbol{\nabla} h) \ , \tag{69}$$

where $\rho_{xx} = D/(D^2 + \psi^2)$, $\rho_{xy} = -\psi/(D^2 + \psi^2)$. The duality of the advection-diffusion formulation of the two-dimensional effective conductivity problem is closely connected with the Keller-Dykhne reciprocity relations.

Equations (68) and (69) are useful to analyse the geometry of the electric field and the current. Specifically, Eqs. (68) and (69) indicate that in the limit of a strong Hall effect, when the Péclet number $P \equiv \langle(\psi - \langle\psi\rangle)^2\rangle^{1/2} / \langle D\rangle$ is large, the angles between the isopotentials ($\phi = \text{const}$), the current lines ($h = \text{const}$), and the isolines of $\psi(x, y)$ are all of order $P^{-1} \ll 1$. That is, these lines approximately coinside almost everywhere.

One can use the advection-diffusion analogy to calculate the effective conductivity of a Hall medium with the help of the results of Sec. 3. The enhanced diffusion then corresponds to an anomalous resistance [19,20]. One of practically interesting applications of this theory is the calculation of the resistance of plasma openning switches. Chukbar and Yankov [21] call this effect the "electron MHD resistance" because the underlying plasma dynamics is described by the equations of electron magnetohydrodynamics [22].

The inverse use of the advection-diffusion analogy can be demonstrated on the example of the exact result (52)–(53) for the effective conductivity of a symmetrical two-phase system. Then (52) is the effective diffusivity in flow of infinitesimally narrow velocity jets separating the domains I and II. Formula (53) can be rewritten as $\psi^* = (1/2)(\psi_1 + \psi_2) - (1/2)(\psi_1 - \psi_2)(D_1 - D_2)/(D_1 + D_2)$. Upon comparing this expression with Eq. (67) we conclude that the effective diffusivity tensor in the flow with the discontinuous stream function $\psi(x, y)$ and the inhomogeneous molecular diffusivity $D(x, y)$ has not only the usual symmetric part (52), but also the antisymmetric part

$$\widehat{\mathbf{D}}^a_{\text{eff}} = -\frac{\psi_1 - \psi_2}{2}\frac{D_1 - D_2}{D_1 + D_2}\widehat{\epsilon}\,. \tag{70}$$

One can call this the "diffusive Hall effect." The nature of this effect is demonstrated

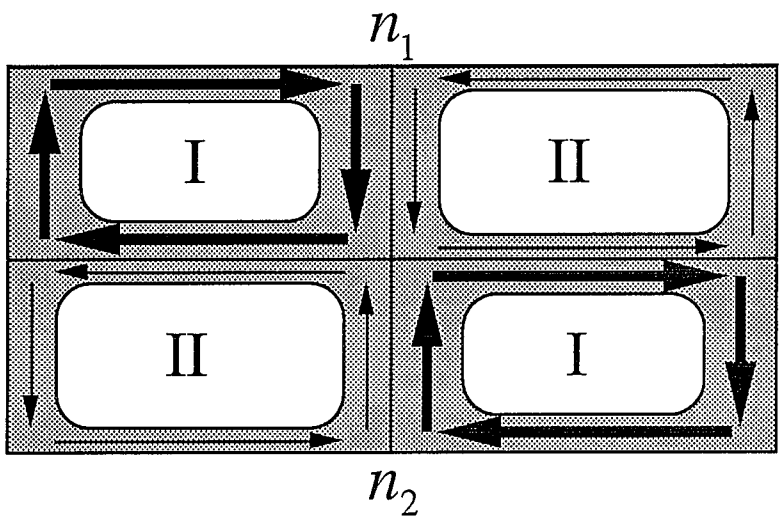

Figure 8: The origin of the diffusive Hall effect on the example of periodic convection cells. If in the cells I the molecular diffusion is greater than in cells II, then the diffusive boundary layers are wider in I. Then, at the top the concentration n_1 is advected more to the right than to the left, whereas n_2 at the bottom is advected leftwise. Thus the resulting flux has a horizontal (Hall) component proportional to the difference $n_1 - n_2$.

in Figure 8. It is not yet clear whether the diffusive Hall effect has useful applications.

7. Conclusions

The author tried to demonstrate that percolation theory has surprisingly many applications in many areas of physics even beyond such traditional areas as semiconductors, phase transitions, or porous media. The multidisciplinary survivability of percolation is due to yet poorly appreciated universality of critical behavior, that is, the structural stability of the percolation exponents under moderate modifications of the model itself.

By introducing increasing changes, most notably correlations between the underlying random objects, the percolation behavior will be finally driven out of its standard universality class. Even then there exists another, *continuous universality*, where the critical exponents continuously depend on the Hölder exponent H describing the algebraic correlations or the correlator of a random potential.

A renormalization-type approach of the *separation of scales* [13] predicts the following fractal dimension of an isoline of a random potential with the power-law spectrum $\psi_\lambda \propto \lambda^H$:

$$\tilde{d}_h(H) = \frac{10 - 3H}{7}, \quad -3/4 < H < 1 \; . \tag{71}$$

Expression (71) goes over to the universal monoscale value $d_h = 7/4$ at $H = -1/\nu = -3/4$, which persists for $H < -3/4$. However, the numerical study of Avellaneda *et al.* [44] undertaken for $H = 1/2$ questioned the formula (71), because the measured fractal dimension $\tilde{d}_h(H) = 1.27715$ was found to be away from the theoretical value of 1.214... by more than the reported numerical error. So the statistical topography of correlated fields needs additional work in both theory and computation.

Acknowledgements

I am grateful to A.M. Dykhne for stimulating discussions and to A.A. Chernikov and M. Avellaneda for communicating their unpublished results. This work was supported by the U.S. Department of Energy.

References

[1] D. Stauffer, *Phys. Rep.* *V* **54** 2 1979.

[2] D. Stauffer, *Introduction to percolation theory* Taylor and Francis, London 1985.

[3] B.I. Shklovskii and A.L. Efros, *Electronic properties of doped semiconductors* Springer, New York 1984.

[4] M.B. Isichenko, *Rev. Mod. Phys.* *V* **64** 961 1992.

[5] P.W. Anderson, *Phys. Rev.* *V* **109** 1492 1958.

[6] J.M. Ziman, *Models of disorder* Cambridge University Press, New York 1979.

[7] R. Zallen, *The physics of amorphous solids* Wiley, New York 1983.

[8] S. Havlin and D. Ben-Avraham, *Adv. Phys.* *V* **36** 695 1987.

[9] A.B. Harris, *Phil. Mag. V* **B56** 833 1987.

[10] A. Kapitulnik, A. Aharony, G. Deutscher, and D. Stauffer, *J. Phys. V* **A16** L269 1984.

[11] H. Saleur and B. Duplantier, *Phys. Rev. Lett. V* **58** 2325 1987.

[12] A. Weinrib, *Phys. Rev. V* **B29** 387 1984.

[13] M.B. Isichenko and J. Kalda, *J. Nonlinear Science V* **1** 255 1991.

[14] M.B. Isichenko, J. Kalda, E.B. Tatarinova, O.V. Telkovskaya, and V.V. Yankov, *Sov. Phys. JETP V* **69** 517 1989.

[15] A.V. Gruzinov, M.B. Isichenko, and J. Kalda, *Sov. Phys. JETP V* **70** 263 1990.

[16] M.B. Isichenko and J. Kalda, *J. Nonlinear Science V* **1** 375 1991.

[17] V.E. Kravtsov, I.V. Lerner, and V.I. Yudson, *Sov. Phys. JETP V* **64** 336 1986.

[18] S.A. Trugman, *Phys. Rev. V* **B27** 7539 1983.

[19] Yu.A. Dreizin and A.M. Dykhne, *Sov. Phys. JETP V* **36** 127 1973.

[20] M.B. Isichenko and J. Kalda, *Sov. Phys. JETP V* **72** 126 1991.

[21] K.V. Chukbar and V.V. Yankov, *Sov. Tech. Phys. V* **58** 2130 1988.

[22] A.S. Kingsep, K.V. Chukbar, and V.V. Yankov, *Reviews of Plasma Physics (edited by B.B. Kadomtsev)* (Consultants Bureau, New York, vol. 16, p. 243 1990.

[23] M.N. Rosenbluth, H.L. Berk, I. Doxas and W. Horton, *Phys. Fluids V* **30** 2636 1987.

[24] M.B. Isichenko, W. Horton, D.E. Kim, E.G. Heo, and D.-I. Choi, *Phys. Fluids V* **B4** 3973 1992.

[25] A.A. Chernikov and A.V. Rogalsky, "Diffusion on stochastic webs near the percolation threshold," to be published .

[26] M.B. Isichenko and W. Horton, *Comments on Plasma Phys. Contr. Fusion V* **14** 249 1991.

[27] M. Rosenbluth, R.Z. Sagdeev, J.B. Taylor and G.M. Zaslavsky, *Nucl. Fusion V* **6** 297 1966.

[28] A.B. Rechester and M. Rosenbluth, *Phys. Rev. Lett. V* **40** 38 1978.

[29] B.B. Kadomtsev and O.P. Pogutse, *Plasma Physics and Controlled Nuclear Fusion Research (Proc. 7th Int. Conf., Innsbruck)* IAEA, Vienna, 1979, vol. I, p. 649 1979.

[30] J.A. Krommes, *Prog. Theoret. Phys. Suppl. V* **64** 137 1978.

[31] K. von Klitzing, G. Dorda and M. Pepper, *Phys. Rev. Lett. V* **45** 494 1980.

[32] K. von Klitzing, *Rev. Mod. Phys. V* **58** 519 1986.

[33] R.B. Laughlin, *The quantum Hall effect* Springer, New York, p. 233 (R.E. Prange and S.M. Girvin, eds.) 1990.

[34] R.W. Rendell and S.M. Girvin, *Phys. Rev. V* **B23** 6610 1981.

[35] M.B. Isichenko and J. Kalda, *J. Moscow Phys. Soc. V* **2** 55 1992.

[36] D.C. Tsui, H.L. Störmer and A.C. Gossard, *Phys. Rev. Lett. V* **48** 1559 1982.

[37] A.M. Dykhne, *Sov. Phys. JETP V* **25** 170 1967.

[38] J. Keller, *J. Math. Phys. V* **5** 548 1964.

[39] A.M. Dykhne, *Sov. Phys. JETP V* **32** 63, 348 1971.

[40] B.Ya. Balagurov, *Sov. Phys. Solid State V* **20** 1922 1978.

[41] M.B. Isichenko, *Plasma Phys. Contr. Fusion V* **33** 795 1991.

[42] A.M. Chang, *The quantum Hall effect* Springer, New York, p. 175 (R.E. Prange and S.M. Girvin, eds.) 1990.

[43] E.B. Tatarinova, P.A. Kalugin and A.V. Sokol, *Europhys. Lett. V* **14** 773 1991.

[44] M. Avellaneda, F. Elliott, Jr. and C. Apelian, "Trapping, percolation and anomalous diffusion in a two-dimensional random field," to be published .